The Journal of Chemical Physics

RESEARCH ARTICLE | JULY 11 2023

Boltzmann's equation at 150: Traditional and modern solution techniques for charged particles in neutral gases

G. J. Boyle ; P. W. Stokes ; R. E. Robson ; R. D. White

J. Chem. Phys. 159, 024306 (2023)
https://doi.org/10.1063/5.0153973

AIP Publishing

The Journal of Chemical Physics ARTICLE pubs.aip.org/aip/jcp

Boltzmann's equation at 150: Traditional and modern solution techniques for charged particles in neutral gases

Cite as: J. Chem. Phys. 159, 024306 (2023); doi: 10.1063/5.0153973
Submitted: 12 April 2023 • Accepted: 21 June 2023 •
Published Online: 11 July 2023

G. J. Boyle,[a] P. W. Stokes,[b] R. E. Robson, and R. D. White

AFFILIATIONS

James Cook University, College of Science and Engineering, Townsville, Australia

[a]**Author to whom correspondence should be addressed:** Gregory.Boyle@my.jcu.edu.au
[b]**Current address:** The Department of Medical Physics, Townsville University Hospital, Townsville, Australia.

ABSTRACT

Seminal gas discharge experiments of the late 19th and early 20th centuries laid the foundations of modern physics, and the influence of this "golden era" continues to resonate well into the 21st century through modern technologies, medical applications, and fundamental scientific investigations. Key to this continuing success story has been the kinetic equation formulated by Ludwig Boltzmann in 1872, which provides the theoretical foundations necessary for analyzing such highly non-equilibrium situations. However, as discussed here, the full potential of Boltzmann's equation has been realized only in the past 50 years or so, with modern computing power and analytical techniques facilitating accurate solutions for various types of charged particles (ions, electrons, positrons, and muons) in gases. Our example of thermalization of electrons in xenon gas highlights the need for such accurate methods—the traditional Lorentz approximation is shown to be hopelessly inadequate. We then discuss the emerging role of Boltzmann's equation in determining cross sections by inverting measured swarm experiment transport coefficient data using machine learning with artificial neural networks.

I. INTRODUCTION

In an article entitled "Weitere Studien uber das Wärmegleichgewicht unter Gasmolekülen" ("Further investigations on the thermal equilibrium of gas molecules") published in 1872,[1] Ludwig Boltzmann (memorial pictured in Fig. 1) proposed a kinetic equation describing the evolution of a non-equilibrium classical gas through a distribution function $f(\boldsymbol{r},\boldsymbol{c},t)$ in phase space $(\boldsymbol{r},\boldsymbol{c})$, where $\boldsymbol{r}$ is the position and $\boldsymbol{c}$ is the velocity, which has had a profound influence on many branches of physics.

The centenary of Boltzmann's seminal work was celebrated by a comprehensive collection of articles of both scientific and biographical nature.[2] The present article, which has been written to mark the sesquicentenary of Boltzmann's equation, focuses on developments since then, that is, in the past 50 years or so.

Boltzmann's kinetic equation may be written in the generic form as

$$\left(\frac{\partial}{\partial t}+\boldsymbol{c}\cdot\nabla+\frac{\boldsymbol{F}}{m}\cdot\frac{\partial}{\partial \boldsymbol{c}}\right)f(\boldsymbol{r},\boldsymbol{c},t)=\left(\frac{\partial f}{\partial t}\right)_{\rm col}, \tag{1}$$

where $\boldsymbol{F}$ is the external force acting on a species of mass m. The collision term $\left(\frac{\partial f}{\partial t}\right)_{\rm col}$ involves an integral operator and is generally nonlinear in f. In its original form, it represents the rate of change of f due to classical, binary, elastic collisions between the constituent species. Boltzmann's equation has been extended to include inelastic collisions by Wang Chang *et al.*[3] and has been generalized to quantum, relativistic, and condensed matter systems (see Ref. 4 for a review). Put simply, the task is to solve (1) and then find the quantities of physical interest, such as particle density, average energy, and currents, by taking appropriate velocity "moments" (integrals over $\boldsymbol{c}$) of $f(\boldsymbol{r},\boldsymbol{c},t)$. However, the nature of $\left(\frac{\partial f}{\partial t}\right)_{\rm col}$ makes this a challenging proposition.

The emergence of Boltzmann's equation preceded a period of intense study of electrical discharges in gases at the end of the nineteenth and early twentieth centuries, sometimes referred to as the "golden era" of physics. It led, for example, to the discovery of the electron by J. J. Thomson and to the confirmation by Franck and Hertz of the Bohr model of quantization of the atom.

FIG. 1. Memorial headstone of Ludwig Boltzmann in the Vienna Cemetery (Source: M. Hildebrandt).

However, it took some time for the potential of Boltzmann's equation for this field to be recognized, first by Pidduck[5] (1917) in the context of light particles (electrons) and the Lorentz approximation. Since then, Boltzmann's equation has come to be acknowledged as the first choice for analyzing charged particles in gases and condensed matter. Examples of applications range from fundamental studies of electron and ion swarms in gases to investigations of the plasma–surface interactions that underpin the microelectronics industry to positron emission tomography. All such investigations required an accurate solution of Boltzmann's equation, which has been made possible over the past 50 years or so through great improvements in computing power. This era forms the focus of the present article. The discussion is, however, limited to the case of dilute charged particles in a background medium at equilibrium, where the collision term is linear in f.

This article represents the key developments that have been made since the centenary publication[2] (Sec. II) and the emerging methods that promise to define the coming era (Sec. III). We begin this work in Sec. II A by outlining a unified approach to the solution of linear Boltzmann's equation, valid for charged particles of all masses (electrons, positrons, muons, and ions), which avoids the limitations of the traditional approach of using a two-term representation of f. We then consider a situation where the solution procedure is greatly simplified in Sec. II B, the thermalization of light particles in a gas subject to an electric field. Here, the convergence of the representation of f in Legendre polynomials, during both the thermalization process and the final steady state, is compared, with surprising results. The next 50 years will be marked by new computational techniques and architectures and further increase computing power, and in Sec. III, we outline one important application from the emerging field of machine learning, i.e., the use of artificial neural networks to determine scattering cross sections from swarm measurements. The fast and robust solution procedures for Boltzmann's equation described in Sec. II B are leveraged here for the generation of the artificial neural network training dataset.

II. KEY DEVELOPMENTS SINCE THE CENTENARY

In this article, we consider dilute swarms of charged particles (electrons, positrons, ions, and muons) of mass m and number density n in a neutral gas of number density n_0 in equilibrium at temperature T_0. In this case, $n \ll n_0$, collisions between charged particles are negligible, and the collision operator of (1) is approximately *linear* in the charged particle velocity distribution function $f(\boldsymbol{c})$, i.e.,

$$\left(\frac{\partial f}{\partial t}\right)_{\text{col}} \approx -J(f, f_0) = -\int \left[f(\mathbf{c}) f_0(\mathbf{c}_0) - f(\mathbf{c}') f_0(\mathbf{c}_0')\right] g\sigma(g,\chi) d\hat{\mathbf{g}}' d^3 c_0, \quad (2)$$

where Boltzmann's original collision operator describes elastic collisions between structure-less charged particles and neutrals governed by a scattering cross section $\sigma(g,\chi)$. Here, $\mathbf{g} = \mathbf{c} - \mathbf{c}_0$ is the relative velocity, χ is the scattering angle in the center-of-mass frame, primes denote post-collision quantities, and $d\hat{\mathbf{g}}'$ is the element of solid angle into which scattering takes place. In this description, the neutrals have a Maxwellian distribution function $f_0(\mathbf{c}_0)$ at temperature T_0. The neutral number density n_0 can be scaled out of Eqs. (1) and (2) such that the solution and transport properties solely depend on "reduced" variables, e.g., the reduced electric field E/n_0 or reduced time $n_0 t$. It is emphasized that this expression for $J(f, f_0)$ applies to *all* charged particles, regardless of the magnitude of their mass m relative to the neutral mass m_0. However, for light particles, such as electrons and positrons, where $m/m_0 \ll 1$, it has long been known that $J(f, f_0)$ may be approximated in the differential form to first order in m/m_0 (see, e.g., the work of Chapman and Cowling[6] for a derivation), which, along with an assumption of quasi-isotropy in velocity space (Lorentz approximation) based on small elastic collisional energy transfer $\sim 2\, m/m_0$, greatly simplifies the solution of (1).

Equation (2) can be readily generalized to allow for excitation of neutral internal energy levels through inelastic processes via the collision operator of Wang Chang *et al.*[3] This too can be approximated, if desired, for light particles, e.g., contributions from inelastic collisions are usually approximated to zero order in m/m_0 to yield the finite-difference form of Frost and Phelps.[7,8] However, since energy transfer is not necessarily small in inelastic collisions, any assumption of quasi-isotropy in velocity space and the use of the Lorentz approximation are subject to doubt. It is emphasized that the collision operators of Boltzmann and Wang Chang *et al.* subsume these traditional, approximate forms, and thus, a general solution of (1), avoiding the Lorentz approximation, offers a way of treating charged particles of all masses, avoiding the approximations mentioned above.

The calculation of the phase-space distribution function $f(\boldsymbol{r}, \boldsymbol{c}, t)$ from (1) can be broadly separated into direct solutions,[9–11] path-integral methods,[12–15] and expansion methods,[16–21] each with their own advantages and disadvantages. Naturally, there also exist many approaches that combine techniques from these general categories. An important alternate method to calculate $f(\boldsymbol{r}, \boldsymbol{c}, t)$ without solving (1) can be done with particle simulation methods (see Ref. 22 for reviews). These are outside the scope of this work, beyond noting that the deterministic solution of Boltzmann's equation and particle simulations are equivalent.[23,24] Expansion methods encompass a

particularly wide set of approaches, from the implicit use via orthogonal polynomial quadrature[25–27] to using complex, physics- and symmetry-informed functions.[28–30] Many of the numerical methods have been replicated from the field of fluid dynamics since analogies with kinetic theory are clear. For example, the use of spectral techniques in velocity space developed in fluid mechanics[31] has been applied and extended to Boltzmann's equation.[32–34]

Ion kinetic theory was discussed in a seminal paper by Wannier[35] (1953), but the modern era might be said to have really begun with the series of papers commencing in 1975 by Viehland, Mason, and collaborators, who developed a solution method of Boltzmann's equation for dilute ions in gases in electric fields of arbitrary strength.[36–38] In 1979, Lin *et al.*[16] developed a general, but somewhat different solution technique, based on the tensor formalism of Kumar.[39–40] Although the procedure is applicable to charged particles of any mass, initial investigations focused on the validity of the Lorentz approximation for electrons. The resulting expansion coefficients have a clear physical meaning, e.g., drift velocities and diffusion coefficients. This theory was later generalized by Robson and Ness who formally decomposed Boltzmann's equations into spherical harmonics.[17,41] Subsequently, the method has been generalized to deal with electron, positron, muon, and ion swarms in gases and condensed matter,[17,41–49] in both electric and magnetic fields.

Much of the foundational multi-term studies focused on electron transport. Key multi-term theories for charged particle swarms under the action of an electric field were developed by Pitchford and Phelps,[50,51] McMahon,[52] Segur *et al.*,[53,54] and Yachi *et al.*,[55] only the last two of which are valid for non-conservative collisions. Ness[42,56] proposed a general formalism for solving Boltzmann's equation for charged particles in electric and magnetic fields, which was further developed by White *et al.*[45,57] Multi-term solutions of the Boltzmann equation for the temporal relaxation of electrons in the presence of both electric and magnetic fields, for a range of experimental configurations, were subsequently developed independently at Greifswald[58–61] and at JCU.[44,45,49,62] Despite the existence of these rigorous multi-term methods, the use of the traditional two-term expansion method in swarm and plasma models is still prevalent.[63]

A. Toward a unified approach to solving Boltzmann's equation for charged particles of arbitrary mass

Expansion methods for the solution of Boltzmann's equation are well-established in the literature not only for charged particles in gases but also for neutron transport (see, e.g., the work of Williams,[64] particularly Chap. 11). We start from the decomposition

$$f(\boldsymbol{r},\boldsymbol{c},t) = \sum_{l=0}^{l_{\max}} \sum_{m=-l}^{l} f_m^{(l)}(\boldsymbol{r},c,t) Y_m^{[l]}(\hat{\boldsymbol{c}}), \tag{3}$$

where $Y_m^{[l]}$ are spherical harmonics, combined with a speed-space decomposition,

$$f_m^{(l)}(\boldsymbol{r},c,t) = \sum_{v=0}^{v_{\max}} F_m^{(vl)}(\boldsymbol{r},t)\Phi_{vl}(c), \tag{4}$$

where $\Phi_{vl}(c)$ are speed-space basis functions, e.g., products of a Maxwellian weighting function and Sonine polynomials of degree v, but this is by no means the only possibility. Alternatively, the coefficients $f_m^{(l)}(\boldsymbol{r},c,t)$ can be represented at a discrete number of points in speed space, though this can be argued to be closely related[27,64] to the decomposition (4). The coefficients $F_m^{(vl)}(\boldsymbol{r},t)$ can be related to physically measurable quantities, such as density and mean energy.[16] The parameters $v_{\max}$ and $l_{\max}$ are integer parameters, which are progressively increased until some convergence criterion is met. The choice of the basis function is particularly important for achieving convergence of (4). For certain potentials, convergence issues are well known.[15] Finally, the space-time dependence of the coefficients $F_m^{(vl)}(\boldsymbol{r},t)$ can be further represented in terms of a density gradient expansion to make contact with the traditional hydrodynamic transport coefficients (see, e.g., Refs. 4, 17, and 41 for details).

By choosing the well-known Burnett functions[28–30] for the basis functions in (3) and (4), substitution into (1) leads to the following infinite set of partial differential equations for $F_m^{(vl)}(\boldsymbol{r},t)$:[4]

$$\sum_{v'=v,v\pm1}\sum_{l'=l,l\pm1}\sum_{m'=l'}^{l'} \left\{\delta_{v'l'm';vlm}\frac{\partial}{\partial t} + \frac{1}{\alpha}(vlm|\boldsymbol{D_1}|v'l'm')\cdot\nabla - \alpha\,(vlm|\boldsymbol{D_2}|v'l'm')\cdot\frac{\boldsymbol{F}}{m} + (vlm|\boldsymbol{J}|v'l'm')\right\} nF_{m'}^{(v'l')}(\boldsymbol{r},t) = 0, \tag{5}$$

where the parameter α is related to a Maxwellian weight function and n is the number density. The quantities $(vlm|\boldsymbol{D_i}|v'l'm')$ $(i = 1,2)$ are "matrix elements" of the operators $\boldsymbol{c}$ and $\frac{\partial}{\partial \boldsymbol{c}}$, respectively, in the Burnett function basis, and similarly, $(vlm|J|v'l'm') = J^l_{vv'}\delta_{mm'}$ represents the matrix elements of the collision operator. These matrix elements are then calculated using the Talmi transformation,[39] and full details can be found in the work of Lin *et al.*[16] One important alternative that deserves mention is the work of Konovalov *et al.*,[21] which avoided the mass-ratio expansion all-together by directly employing Lebedev quadratures over velocity and scattering angles.

Regardless of the choice of basis functions or the solution method for decompositions (3) and (4), the collision operator can be represented by an expansion in terms of $m/(m+m_0)$.[40] For present purposes, it suffices to know that

$$J^l_{vv'} = \sum_{p=0}^{p_{\max}} \left(\frac{m}{m+m_0}\right)^p J^l_{vv'}(p), \tag{6}$$

where $p_{\max}$ is an integer parameter, which can be increased until some desired accuracy criterion is met. The number of terms required in (6) increases with the mass ratio, as illustrated below.

We summarize the solution procedure for (3)–(6):

1. Choose a basis function set $\Phi_{vl}(c)$ and truncation limits, i.e., ($l_{\max}$, $v_{\max}$, and $p_{\max}$) for the summations involving l, v, and p, respectively.
2. Calculate the set of matrix elements for the collision operator, e.g., $J^l_{vv'}(p)$.

3. Substitution of Eqs. (3) and (4) into (1) converts Boltzmann's equation into a set of coupled equations for expansion coefficients $F_m^{(vl)}(\boldsymbol{r},t)$. When using the Burnett function representation, the set of coupled equations is given by (5). These are then solved for $F_m^{(vl)}(\boldsymbol{r},t)$.
4. Increase the truncation limits, either sequentially or collectively, and re-solve for $F_m^{(vl)}(\boldsymbol{r},t)$.
5. Calculate the change in the desired transport properties, e.g., the drift velocity ($v = 0, l = 1$), due to the increase in truncation limits.
6. Increment the truncation limits until some desired accuracy criterion is satisfied, typically 0.1%–1% to be consistent with experimental errors.

The values for the truncation limits are not known *a priori*. The required value of $l_{\max}$ indicates the deviation of the velocity distribution from isotropy, while the required value of $v_{\max}$ indicates the deviation of the speed distribution from the weighting function.

To demonstrate the influence of the mass ratio on transport properties and calculation convergence, we consider a simple hard-sphere elastic scattering model,

$$\sigma_m = 6\ \text{Å}^2, \qquad m_0 = 4\ \text{amu},$$
$$T_0 = 293\ \text{K}, \qquad E/n_0 = 1\ \text{Td}, \tag{7}$$

for ions of different masses. For an electric field only, the velocity distribution function has rotational symmetry about the field direction. In Fig. 2, the velocity distribution function, in the plane containing the electric field, is presented for a selection of mass ratios m/m_0, from 10^{-4} to 10. For $m/m_0 = 10$, the convergence is extremely slow and the contours shown in Fig. 2(f), although qualitatively correct and sufficient for illustrative purposes, are not accurate.[43] As the mass ratio increases, it is clear that the contour dimensions decrease, while also being shifted and elongated in the direction of the field. This is because, as the mass ratio increases, the fractional energy transfer per collision also increases, and thus, the energy available in the preferential forward scattering direction is enhanced, while the energy available in the transverse direction is decreased.

As demonstrated in Fig. 2, increasing the mass ratio leads to increased anisotropy in the velocity distribution, with a shift and elongation of the velocity contours in the direction of the field, and it is to be expected that a greater number of terms in the l- and p-summations are required for convergence. Table I shows the convergence of the mean energy, $\bar{\epsilon}$, drift velocity, W, and transverse and longitudinal diffusion coefficients, $n_0 D_{\mathrm{T}}$ and $n_0 D_{\mathrm{L}}$, respectively, with $l_{\max}$ and $p_{\max}$, for two significantly different mass ratios.

For very light particles (e.g., $m/m_0 = 10^{-4}$, in Table I), it is clear that the two-term approximation $l_{\max} = 1$ is sufficient to obtain accurate transport coefficients within 0.1%, for the simple hard-sphere model. Note that it is well known that the inclusion of inelastic processes can lead to a failure of the two-term approximation, requiring larger $l_{\max}$,[41,63,65] and in Sec. II B, we demonstrate that remarkably large $l_{\max}$ are required during electron thermalization. Truncation at $p_{\max} = 1$ is sufficient to obtain accuracy within 0.1%, as expected, which permits a class of fast Boltzmann's equation solvers for electrons in gases (see Sec. II B).

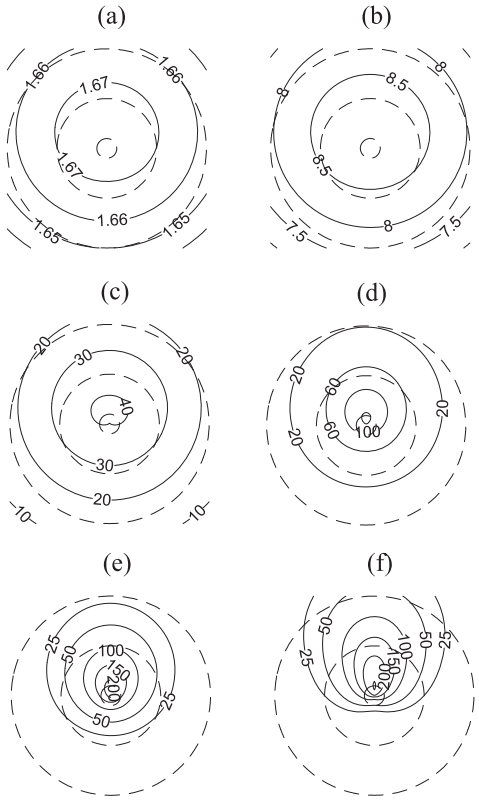

FIG. 2. Contour plots of the velocity distribution functions for various mass ratios for ions in a hard-sphere model gas (7). Contour heights are in units of $\text{eV}^{-3/2}$. The energy scale is indicated by the dashed concentric circular plots of increasing radii referring, respectively, to 0.01, 0.05, and 0.1 eV. (a) $m/m_0 = 10^{-4}$; (b) $m/m_0 = 10^{-3}$; (c) $m/m_0 = 10^{-2}$; (d) $m/m_0 = 10^{-1}$; (e) $m/m_0 = 10^{0}$; and (f) $m/m_0 = 10^{1}$ (source: Adapted from White *et al.*, Comput. Phys. Commun. **142**, 349 (2001). Copyright 2001 Elsevier.

For heavy particles of the same mass as the background particles ($m/m_0 = 1$), the two-term approximation is not sufficient, and $l_{\max} = 3$ is required to achieve the same accuracy. This is due to the increased anisotropy in the velocity distribution function, as shown in Fig. 2. Note that, even when the velocity distribution itself has slow convergence in $l_{\max}$, the transport coefficients corresponding to low-order moments of the velocity distribution (e.g., ϵ and W) can still be well represented. Higher-order moments can be much more sensitive to inaccuracies in the velocity distribution function. For $m/m_0 = 1$, additional terms are also necessary in the collision operator summation, and a $p_{\max} = 4$ truncation is required, along with sufficiently high $l_{\max}$ ($l_{\max} = 5$ is employed in Table I for the $p_{\max}$ convergence), to achieve the 0.1% accuracy. Note that, while a large $p_{\max}$ implies a large $l_{\max}$ for convergence, the converse is, in general, not true.

The situation for muons, whose mass is some 200+ times greater than an electron, is predictably intermediate between electrons and ions. For muons in deuterium gas, it was found that it is necessary to take $p_{\max} = 2$ and $l_{\max} = 3$ or 4 in order to calculate transport properties within an accuracy of 0.1%.[66,67]

TABLE I. Influence of the mass ratio (m/m_0) on convergence in the spherical harmonic expansion (l_{max}) and in the collision matrix expansion (p_{max}) and on selected transport properties for ions in a hard-sphere model gas (7). The results of Monte Carlo (MC) simulation[a] are also given.

m/m_0	l_{max}	$\bar{\epsilon}$ (eV)	W 10^2 m s^{-1}	$n_0 D_T$ 10^{22} m^{-1} s^{-1}	$n_0 D_L$ 10^{22} m^{-1} s^{-1}
10^{-4}	1	0.733 26	56.189	313.31	158.22
	2	0.733 24	56.187	313.20	158.27
	3	0.733 24	56.187	313.20	158.27
	MC	0.733	56.2	313	158
10^{0}	1	0.042 84	3.403	9.77	7.74
	2	0.042 71	3.366	8.92	8.86
	3	0.042 71	3.368	8.94	8.84
	4	0.042 71	3.368	8.94	8.84
	MC	0.042 7	3.37	8.94	8.84
	p_{max}				
10^{-4}	1	0.733 18	56.188	313.20	158.25
	2	0.733 24	56.187	313.20	158.27
	3	0.733 24	56.187	313.20	158.27
	MC	0.733	56.2	313	158
10^{0}	2	0.042 84	3.382	8.98	8.84
	3	0.042 70	3.366	8.93	8.87
	4	0.042 71	3.368	8.94	8.83
	5	0.042 70	3.365	8.95	8.83
	6	0.042 71	3.368	8.94	8.84
	7	0.042 71	3.368	8.94	8.84
	MC	0.042 7	3.37	8.94	8.84

[a]Reference 139.

B. Electron thermalization in uniform electric fields: The necessity of multi-term solutions

When considering light particles, such as electrons or positrons, in a neutral background gas, only the first-order mass-ratio contribution to expansion (6) is required, and thus, the collision operators greatly simplify.[6–8] Furthermore, under certain symmetry conditions, such as the plane-parallel geometry considered in this section, the spherical harmonics in (3) reduce to Legendre polynomials such that

$$f(\boldsymbol{c}) = \sum_{l=0}^{l_{max}} f_l(c) P_l(\mu), \tag{8}$$

where $\mu = \hat{\boldsymbol{F}} \cdot \hat{\boldsymbol{c}}$ and P_l is the lth Legendre polynomial.

A class of fast and robust Boltzmann's equation solvers have been developed that represent the speed-space (or equivalently, the energy-space) using a finite-difference discretization[58,61,68–72] instead of as an expansion in orthogonal bases functions, thereby avoiding the sensitivity of weight function parameter choices and convergence issues for non-Maxwellian distributions. These Boltzmann's equation solvers have been utilized for a wide range of applications involving electrons[59,60,72–76] and positrons[77–79] and are also leveraged in Sec. III. The two-term code BOLSIG+[69] deserves special mention, as it is widely used by the plasma community for calculating rate coefficients, etc., often in connection with the extensive cross-sectional database LXCat,[80,81] in situations where a two-term approximation is assumed to be suitable.

A striking breakdown of the two-term approximation can be seen during the thermalization of electrons subject to uniform electric fields. Typically, the time taken for an electron swarm in a weakly ionized medium to high-pressure plasma (0.01–5 bars) to reach a state of equilibrium with an applied electric field is very short ($<10^{-9}$ s). However, the development of extremely fast pulsed nanosecond discharge plasmas[82] has called into question the validity of using steady-state Boltzmann's equation solver for deducing the velocity distribution function and transport properties. In the work of Boyle *et al.*,[74] time-dependent Boltzmann's equation was numerically solved for electrons in xenon gas subject to an instantaneously applied electric field to follow the energy distribution function (and associated transport coefficients) as it evolves from an initial room-temperature Maxwellian distribution toward the steady-state. Although the focus was to calculate thermalization times, one of the key findings was that a surprisingly large number of Legendre polynomial terms (l_{max}) was required for the transport coefficients to converge during the thermalization, in contrast to the low number required in the steady-state. The evolution of the energy distribution function and transport coefficients for electrons in xenon with an initial thermal Maxwellian distribution (T_0 = 293 K) subject to an E = 1000 Td electric field is explored in Figs. 3 and 4 for various choices of l_{max}.

In Fig. 3, the (normalized) f_0 distribution is shown for a selection of times for l_{max} = 1, 15, and 31, respectively. The reduced times are given in units of ps amagat, where 1 amagat ≈ 44.615 mol m^{-3}. The 2-term (l_{max} = 1) f_0 distribution displays extreme

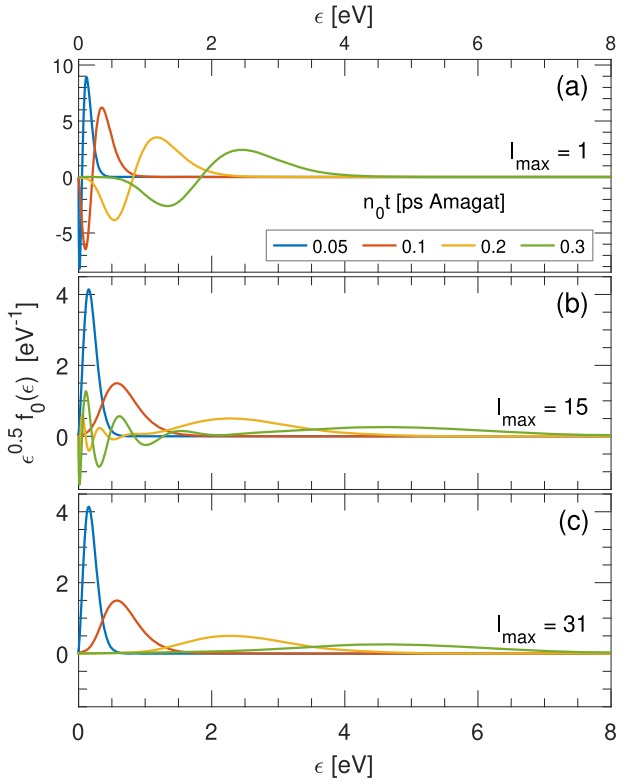

FIG. 3. Energy distribution function component, $\epsilon^{1/2} f_0(\epsilon)$, for electrons in xenon gas subject to a reduced electric field E/n_0 = 1000 Td at select reduced times $n_0 t$ = 0.05, 0.1, 0.2, and 0.3 ps amagat. The initial distribution is a thermal Maxwellian at T_0 = 293 K. Simulations have been performed using (a) 2-term (l_{max} = 1), (b) 16-term (l_{max} = 15), and (c) 32-term (l_{max} = 31) approximations.

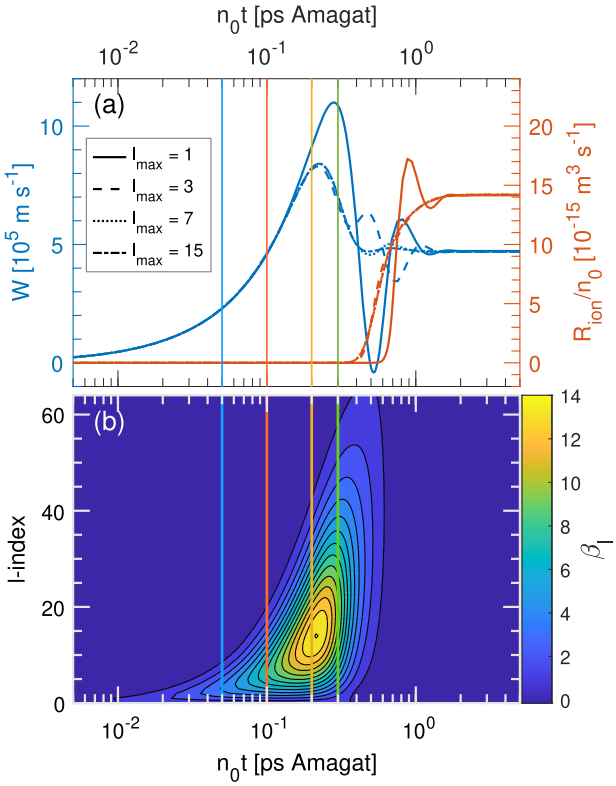

FIG. 4. Temporal evolution of (a) the drift velocity W (left) and reduced ionization rate R_{ion}/n_0 (right) for 2-, 4-, 8-, and 16-term approximations and (b) the relative weighting β_l, given in (9), of the Legendre components in the 64-term approximation. The conditions are the same as those in Fig. 3, with the (color-coded) vertical lines indicating the same reduced times as the energy distribution function profiles.

oscillations and non-physical behavior for all of these times. As discussed in Sec. II A, the failure of the 2-term approximation indicates a significantly anisotropic velocity distribution. The 16-term (l_{max} = 15) f_0 distribution behaves more reasonably; however, oscillations and non-physical behavior are still exhibited for low energies at times above $n_0 t$ = 0.2 ps amagats. Including 32-terms (l_{max} = 31) in the Legendre expansion is sufficient to suppress the oscillatory behavior and to clearly demonstrate the expected increase in mean energy and energy-spread of the electron swarm with time.

In Fig. 4(a), the drift velocity (W) and reduced ionization rate (α_{ion}/n_0) are shown for l_{max} = 1, 3, 7, and 15. The wild oscillations observed in the f_0 distributions at low l_{max} are reflected in swarm transport coefficients. However, only eight terms (l_{max} = 7) are required to obtain converged values within ≈1% for both the drift velocity and the reduced ionization rate, further demonstrating that some non-converged behavior in velocity distributions is not necessarily reflected by low-order transport coefficients. Using 16 terms gives results <0.1% of the converged values. It is clear in Fig. 4(a) that each of the profiles converges to the same values at large times, indicating that a two-term approximation is sufficient to represent the steady-state.

Finally, the contour plot in Fig. 4(b) illustrates the importance of each Legendre component in l_{max} = 63 term simulation, where

$$\beta_l = \frac{\int_0^\infty d\epsilon\ \epsilon^{1/2} f_l(\epsilon)}{\int_0^\infty d\epsilon\ \epsilon^{1/2} f_0(\epsilon)} \tag{9}$$

represents the relative weight of each Legendre term f_l with respect to f_0. Between $n_0 t \approx 0.05 - 0.5$ ps amagat, 10–30 terms are very important, and even f_l values as high as l = 63 have similar weight to f_0. This indicates that the velocity distribution is extremely anisotropic at these times, demonstrating "beam-like" behavior, i.e., a velocity distribution in which all of the particles are essentially traveling in the forward direction. At large times, the energy distribution once again becomes mostly isotropic, i.e., where only a few low-order l terms are important, justifying a low-term expansion when investigating steady-state conditions. The times corresponding to the f_0 distributions in Fig. 3 are indicated by the color-coded vertical lines. At $n_0 t$ = 0.05 and 0.1 ps amagat, ~10–20 Legendre terms are important, which is consistent with the problematic behavior demonstrated by the f_0 profiles for l_{max} = 1 and well-behaved profiles for l_{max} = 15 and 31. At $n_0 t$ = 0.2 and 0.3 ps amagat, the β_l parameter peaks at a one-index of ~15–20, which is reflected in

the breakdown of the corresponding f_0 profiles for $l_{max} = 15$. The peak in the β_l parameter also approximately coincides with the initial departure of low-l_{max} drift velocity calculations away from the converged values, exemplified by the $l_{max} = 1$ case, as shown in Fig. 4(a). Note that the errors induced in the transport coefficients propagate in time significantly beyond the time at which the (converged) energy distribution is once again quasi-isotropic.

We have also performed a similar investigation for helium and observed more extreme behavior with even higher l_{max} (>128) required for convergence throughout the thermalization.[83] At some point, it may be more practical to discretize the velocity space directly, rather than use the Legendre polynomial expansion representation. Given the widespread use of the two-term approximation in plasma modeling, it is important to take note of these situations where higher l_{max} are critical.[63,65,84]

III. THE INVERSE SWARM PROBLEM: OBTAINING CROSS SECTIONS USING ARTIFICIAL NEURAL NETWORKS

Fundamental to plasma physics applications is the availability of accurate and complete cross-sectional information.[85] Direct information about individual scattering processes on the microscopic level can be provided by the experiment (e.g., crossed beam[86]) and theory (e.g., convergent close-coupling[87–90]). Conversely, swarm experiments[65,91–93] provide macroscopic information about ensemble behavior and thereby provide an indirect assessment of the accuracy and self-consistency of the full cross-sectional set.[85] When the knowledge about the individual scattering cross sections is lacking, one may attempt to "unfold" swarm measurement data to assess the cross section. Indeed, the pioneering attempts at deriving electron scattering cross sections from swarm transport coefficients were made in the 1920s,[94–96] decades prior to the development of modern-day beam-scattering experiments. By either assuming a simplified form of the velocity distribution or numerically solving Boltzmann's equation,[7,97–100] the transport coefficients can be calculated, compared to swarm measurements, and then iteratively adjusted. Due to the degeneracy often inherent in the inverse swarm problem, this process inevitably requires some amount of intuition, particularly when available data are limited.

On account of the tedious nature of this trial and error approach to swarm analysis, a number of automated methods have been proposed.[101–107] In 1991, Morgan[105] successfully used an artificial neural network to determine low-energy, electron-xenon scattering cross sections from drift velocity and characteristic energy measurements. Since Morgan's pioneering investigation, the field of machine learning has exploded in popularity, and combined with increasing computing capabilities, much larger and more powerful models have been developed.[108–113]

Pulsed-Townsend experiments are one of the most important modern techniques for extracting drift, diffusion, and ionization rate information from electron swarms.[91,114–117] In a pulsed-Townsend experiment, a sharp pulse of electrons are subject to a uniform electric field directed between two plane-parallel electrodes. If the experimental setup is such that any spatial gradients are weak (the hydrodynamic regime), then the solutions described in Sec. II B based on Legendre polynomials are applicable, allowing for the use of fast Boltzmann's equation solvers. The development of fast Boltzmann's equation solvers for electrons, coupled with the continual increase in computing power over time, has allowed an entire class of problems involving repeated solutions or iterations to be feasible, e.g., using artificial neural networks.[118–120]

In this section, we consider the application of artificial neural networks to determining scattering cross sections from pulsed-Townsend-derived transport coefficients, leveraging fast Boltzmann equation solvers in the generation of the necessary training data.

A. Artificial neural network architecture

Artificial neural networks are highly parameterized mathematical functions capable of universal function approximation.[121,122] By carefully adjusting the parameters (i.e., training), an artificial neural network is capable of nonlinearly mapping between arbitrary input and output vector spaces. In the work of Stokes *et al.*,[76] an artificial neural network for the solution of the inverse swarm problem that learns from the mapping of transport coefficients to cross sections was proposed using a similar architecture to that employed by Morgan.[105] The process is schematically depicted in Fig. 5. The input is a vector of swarm measurements, e.g., bulk drift velocities W and first Townsend ionization coefficients α_T/n_0, along with an energy ϵ, and the output is a vector representing each of the desired cross sections evaluated at the input energy, i.e., $\sigma(\epsilon)$. This architecture allows the neural network to learn a suitable cross-sectional discretization specific to the training data, rather than one that is imposed. Outputting the cross sections at only a single specified energy means that there is only one output neuron per cross section, resulting in a network that is simpler to train, faster to evaluate, and less likely to overspecialize to the training data.

Optimization of the neural network parameters requires extensive training data and a cost function that evaluates the performance of the neural network on the training data. To address the former, a new data augmentation procedure was developed[76] to generate new cross sections by combining the existing cross sections available from the LXCat project.[80,81] Given a pair of LXCat cross sections, $\sigma_1(\epsilon)$ and $\sigma_2(\epsilon)$, of a given type (e.g., electron attachment and

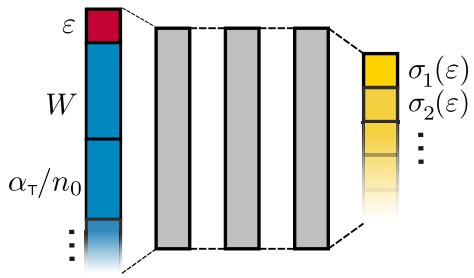

FIG. 5. Symbolic representation of the fully connected artificial neural network used for the regression of selected cross sections, e.g., σ_1 and σ_2 (yellow) as a function of energy ϵ (red), given relevant electron swarm data, e.g., drift velocity W and reduced effective first Townsend ionization coefficient α_T/n_0, measured for a range of reduced electric fields E/n_0 (blue). The network layers (gray) are trained using cross-sectional data chosen carefully, as described in Sec. III A, so as to constrain the derived cross sections to be within the vicinity of their known uncertainties.

ionization), a new physically plausible cross section of the same type is generated via

$$\sigma(\epsilon) = \sigma_1^{1-r}(\epsilon + \epsilon_1 - \epsilon_1^{1-r}\epsilon_2^{r})\sigma_2^{r}(\epsilon + \epsilon_2 - \epsilon_1^{1-r}\epsilon_2^{r}), \tag{10}$$

where ϵ_1 and ϵ_2 are the threshold energies for $\sigma_1(\epsilon)$ and $\sigma_2(\epsilon)$, respectively, and $r \in [0, 1]$ is the mixing ratio. This process can also be performed when $\sigma_1(\epsilon)$ is a specific cross section of interest, e.g., a measured neutral dissociation cross section, to generate variations within its experimental uncertainty. It is here that having a fast Boltzmann equation solver is particularly important, i.e., to calculate the transport coefficients corresponding to each cross section set over a range of reduced electric field strengths. By restricting the range of the training data, the neural network outputs can be implicitly constrained. Finally, to train the artificial neural network, we minimize the mean absolute error,

$$\frac{1}{N}\sum_{i=1}^{N} \|\boldsymbol{y}_i - \boldsymbol{\sigma}(\boldsymbol{x}_i)\|_1, \tag{11}$$

where the index i ranges over the entire set of N training examples $(\boldsymbol{x}_i, \boldsymbol{y}_i)$ and $\boldsymbol{\sigma}(\boldsymbol{x}_i)$ is the associated network cross-sectional prediction. The mean absolute error metric has been chosen for its robustness to outliers in the training data.

B. Inverse swarm problem for electrons in THF

Considerable global effort has gone into determining complete cross-sectional sets for electron transport in biologically important molecules, including water[123] and simple analogs for sugars and DNA bases.[124–127] Tetrahydrofuran (THF)[124,128] is one such analog, a sugar linking phosphate groups in the backbone of DNA. Repeated refinements to the THF cross-sectional set have been made in recent years, both with traditional methods based on expert intuition[75,129,130] and automatically using an artificial neural network.[131] The sparsity of experimental and theoretical data for the neutral dissociation process results in a high degree of degeneracy in the inverse swarm problem. We highlight the suggestion of Casey *et al.*[130] to include two neutral dissociation cross sections, rather than just one as had been done previously. The lower-energy dissociation facilitates agreement with drift velocity measurements, while the higher-energy dissociation is necessary for agreement with Townsend coefficient measurements.[75,130]

To demonstrate the ability of the neural network procedure[76,131] to automatically predict cross sections from swarm data, as well as the importance of the dissociation process to modeling electrons in THF, we have used an artificial neural network under the assumption of (i) a single neutral dissociation process and (ii) two separate neutral dissociation processes. Specifically, the set of cross sections to be determined include the quasielastic (elastic + rotational) momentum-transfer cross section, σ_m, the electron attachment cross section, σ_{att}, the low-threshold neutral dissociation cross section, σ_{nd1}, the high-threshold neutral dissociation cross section, σ_{nd2}, and the ionization cross section, σ_{ion}. The remaining excitation cross sections (e.g., for vibrational excitation and discrete electronic-state excitation) are not included here, as they are considered to be better known, and are instead sourced from the cross-sectional set constructed by de Urquijo *et al.*[75]

For σ_{nd1} and σ_{att}, where guidelines from experiment or theory are absent, the procedure given in (10) is applied directly without explicit constraint, resulting in very large confidence bands. The wide confidence interval band for σ_{nd1} is shown in Fig. 6(a). For the remaining cross sections to be predicted, the training data are explicitly constrained to lie within the vicinity of the known experimental error bars so as to encourage the neural network to also restrict its output in the same way (see the work of Stokes *et al.*[76] for details). The confidence interval band for the σ_{nd2} training data is also shown in Fig. 6(a) and is a much tighter interval than that for σ_{nd1} due to the existence of data from the work of Fuss *et al.*,[126,132] which was determined by subtracting all the known integral cross sections for all open channels from the measured grand total cross section.

Once the separate training cross sections are generated as described above, each is used to replace their counterpart in the original set of de Urquijo *et al.*[75] in order to obtain a proposed full dataset of cross sections for training. The set of predicted THF cross section, including one and two neutral dissociation processes, respectively, is shown in Fig. 6(b). The inclusion of σ_{nd1} shifts σ_{nd2} to higher energies (the threshold energy increases from 5.7 to 7.4 eV) and also increases the peak cross-sectional value by ~20%. σ_{att} is also significantly enhanced in the 1–10 eV range, which agrees better with the literature.[133,134] The profiles for σ_m and σ_{ion} do not differ significantly between including 1 or 2 neutral dissociation processes. The predicted cross sections when assuming two neutral dissociations are necessarily very similar to those in Ref. 131. The minor differences are due to the use of a four-term (rather than two-term) solution of Boltzmann's equation, as well as the inherently random nature of minimizing the cost function (11) via stochastic gradient descent.

The drift velocity W and reduced effective Townsend coefficients α_T/n_0 calculated with these cross-sectional sets are shown in Figs. 7(a) and 7(b), respectively, along with pulsed-Townsend experimental measurements,[75] for electron transport in both pure THF and admixtures of THF in argon. The admixtures of THF range from 1% to 50%, and the argon cross-sectional set from the Biagi v7.1 database[135] has been used for argon calculations. Using admixtures with a well-characterized gas, such as argon, allows us to reduce the potential non-uniqueness in the derived cross sections.

Generally, the inclusion of two neutral dissociation processes improves the agreement of the calculated transport coefficient with measurements, doing so most substantially for the drift velocity, while only slightly improving the agreement for the reduced Townsend coefficient, which appears to be less sensitive to the presence of a low-threshold dissociation process. These results are consistent with previous findings.[130,131] The discrepancies that remain between calculation and measurement suggest that there is room for further improvements to the accuracy and completeness of the electron-THF cross-sectional set. Indeed, Fig. 6 shows a "bump" in σ_{nd1} in the range of 2–20 eV that may be indicative of an intermediate-threshold process that is currently absent from the set, manifesting here only implicitly as a feature in the low-threshold neutral dissociation cross section. Future data-driven investigations could shed further light on this possibility.

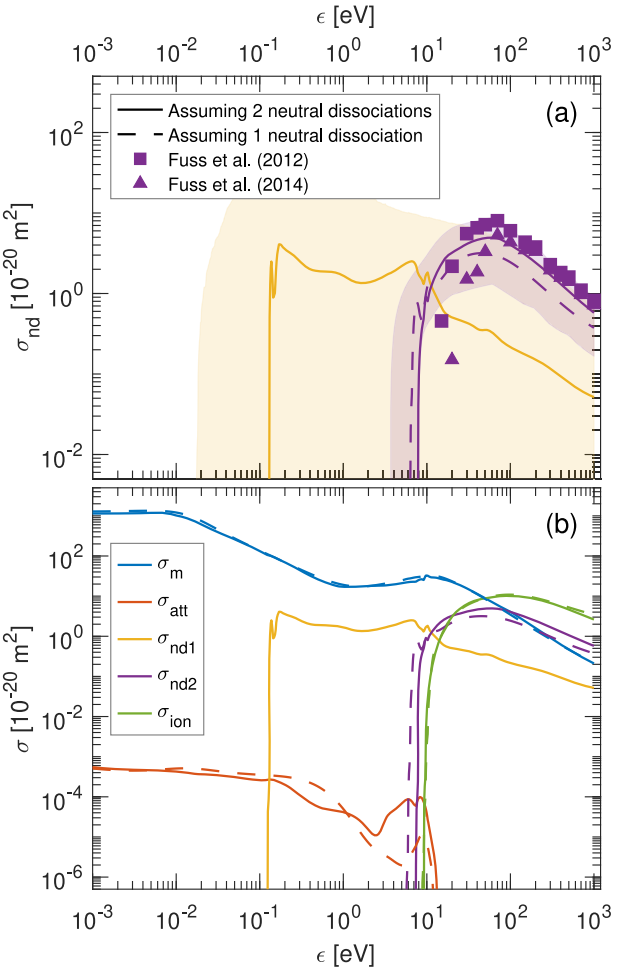

FIG. 6. Cross sections for electron-THF scattering predicted by the artificial neural network from swarm data, assuming two neutral dissociation processes (solid curves) or one neutral dissociation process (dashed curves). (a) Neutral dissociation processes. The shaded intervals indicate the 99% confidence intervals of the training data. (b) The full set of predicted cross sections. The remaining cross sections are considered known and are taken from the work of de Urquijo *et al.*[75]

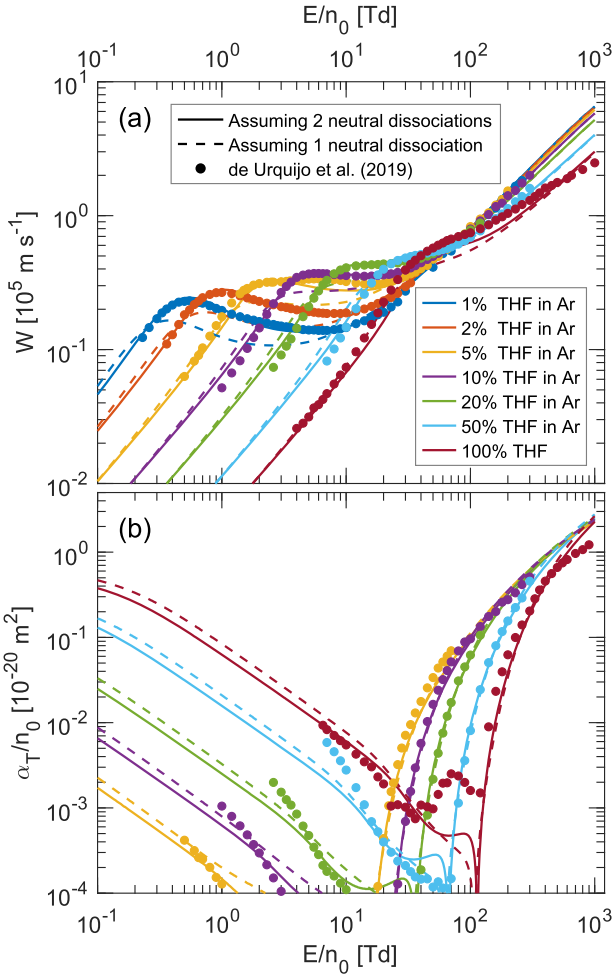

FIG. 7. Simulated transport coefficients for THF-Ar mixtures assuming two neutral dissociation processes (solid curves) or one neutral dissociation process (dashed curves) of (a) flux drift velocity W and (b) reduced effective first Townsend ionization coefficient α_T/n_0 for the neural network refined cross-sectional sets shown in Fig. 6.

IV. SUMMARY

Boltzmann's kinetic equation has proved indispensable in describing a wide range of non-equilibrium phenomena during its 150 years of existence, none more important than in the gas discharge experiments of the type, which characterized the "golden era" of physics, around the late nineteenth and early twentieth centuries, which ushered in the modern era of physics, and whose applications to fundamental science, medicine, and technology continue to resonate well into the twenty-first century. This article focuses on developments over the past 50 years or so in the solution of Boltzmann's equation for dilute charged particles (electrons, positrons, muons, and ions) in a gas in equilibrium, where the advent of modern computing power has obviated the need and, indeed, the desirability for making traditional approximations and assumptions based on particle mass. We give examples to illustrate this point, using a unified technique for solving Boltzmann's equation, valid for electrons, muons, and ions. The limitations of the traditional "two-term" spherical harmonic approximation of the velocity distribution function have long been well-documented for electrons making inelastic collisions with the neutral gas, but in the example presented here, where electrons thermalize in a neutral gas by means of elastic collisions only, it is shown that a very high-order multi-term expansion, up to order 30 or more, is required to attain the desired accuracy. We then turn our attention to a state-of-the-art application of artificial neural networks, i.e., the determination of electron-neutral scattering cross sections by unfolding swarm experiments. These universal function approximators offer an alternative to the tedious trial-and-error approach and can leverage the wealth of existing experimental and theoretical data for training. For the specific case of electrons interacting with tetrahydrofuran,

we have demonstrated how assumptions about the low-energy neutral dissociation cross sections, which lack experimental data, affect the outputs predicted by the artificial neural network. Furthermore, noting the development of physics-informed neural networks,[136,137] the field of machine learning promises a new era of Boltzmann's equation analyses.

Finally, while we naturally wish to highlight the successes of Boltzmann's equation on the occasion of its 150th anniversary, this is not done without some reservation. For example, there is a long-standing controversy surrounding the (e, H_2) system: swarm experimental data cannot be fitted with Boltzmann's equation using the vibrational cross section determined from beam experiments. As explained by Robson *et al.*,[138] one possibility is that a new kinetic equation may be necessary to describe molecular systems, possibly one that avoids key assumptions inherent in Boltzmann's equation, such as instantaneous, local collisions. At the time of writing, this remains an open question.

ACKNOWLEDGMENTS

The authors wish to acknowledge the assistance of D. G. Cocks in providing the Monte Carlo results in Table I and helpful discussions with R. J. Carman, R. P. McEachran, M. J. E. Casey, and D. L. Muccignat. The authors acknowledge the Australian Research Council through its Discovery program (Grant Nos. DP180101655 and DP220101480).

AUTHOR DECLARATIONS

Conflict of Interest

The authors have no conflicts to disclose.

Author Contributions

G. J. Boyle: Conceptualization (equal); Data curation (equal); Formal analysis (equal); Investigation (equal); Writing – original draft (lead); Writing – review & editing (equal). **P. W. Stokes**: Conceptualization (supporting); Data curation (equal); Formal analysis (equal); Investigation (equal); Supervision (supporting); Writing – original draft (supporting); Writing – review & editing (supporting). **R. E. Robson**: Conceptualization (lead); Data curation (equal); Investigation (equal); Methodology (equal); Writing – original draft (equal); Writing – review & editing (equal). **R. D. White**: Conceptualization (equal); Data curation (equal); Formal analysis (equal); Investigation (equal); Supervision (supporting); Writing – original draft (supporting); Writing – review & editing (supporting).

DATA AVAILABILITY

The data that support the findings of this study are available from the corresponding author upon reasonable request.

REFERENCES

[1]L. Boltzmann, "Weitere studien über das wärmegleichgewicht unter gasmolekülen," Wien. Ber. **66**, 275 (1872).
[2]E. Cohen and W. Thirring, *The Boltzmann Equation* (Springer, 1973).
[3]C. S. Wang Chang, G. E. Uhlenbeck, and J. de Boer, in *Studies in Statistical Mechanics*, edited by J. de Boer and G. E. Uhlenbeck (North-Holland, 1964), Chap. The Heat Conductivity and Viscosity of Polyatomic Gases, Vol. II.
[4]R. E. Robson, R. D. White, and M. Hildebrandt, *Fundamentals of Charged Particle Transport in Gases and Condensed Matter* (CRC Press, 2017).
[5]F. B. Pidduck, "The kinetic theory of the motion of ions in gases," Proc. London Math. Soc. 2017, 89.
[6]S. Chapman and T. G. Cowling, *The Mathematical Theory of Non-Uniform Gases: An Account of the Kinetic Theory of Viscosity, Thermal Conduction and Diffusion in Gases* (Cambridge University Press, 1970).
[7]L. S. Frost and A. V. Phelps, "Rotational excitation and momentum transfer cross sections for electrons in H_2 and N_2 from transport coefficients," Phys. Rev. **127**, 1621 (1962).
[8]K. Kumar, H. Skullerud, and R. E. Robson, "Kinetic theory of charged particle swarms in neutral gases," Aust. J. Phys. **33**, 343 (1980).
[9]P. J. Drallos and J. M. Wadehra, "Exact time-dependent evolution of electron-velocity distribution functions in a gas using the Boltzmann equation," Phys. Rev. A **40**, 1967 (1989).
[10]K. Maeda and T. Makabe, "Time-dependent RF swarm transport by direct numerical procedure of the Boltzmann equation," Jpn. J. Appl. Phys. **33**, 4173 (1994).
[11]H. Sugawara, "A computational scheme of propagator method for moment equations to derive real-space electron transport coefficients in gas under crossed electric and magnetic fields," IEEE Trans. Plasma Sci. **47**, 1071 (2019).
[12]P. Kleban and H. T. Davis, "Electron transport in methane gas," Phys. Rev. Lett. **39**, 456 (1977).
[13]G. L. Braglia, "Motion of electrons and ions in a weakly ionized gas in a field. I. Foundations of the integral theory," Beitr. Plasmaphys. **20**, 147 (1980).
[14]H. R. Skullerud and S. Kuhn, "On the calculation of ion and electron swarm properties by path integral methods," J. Phys. D: Appl. Phys. **16**, 1225 (1983).
[15]H. R. Skullerud, "Developments in the kinetic theories of ion and electron swarms in the 1960s and 70s," Plasma Sources Sci. Technol. **26**, 045003 (2017).
[16]S. L. Lin, R. E. Robson, and E. A. Mason, "Moment theory of electron drift and diffusion in neutral gases in an electrostatic field," J. Chem. Phys. **71**, 3483 (1979).
[17]K. F. Ness and R. E. Robson, "Velocity distribution function and transport coefficients of electron swarms in gases. II. Moment equations and applications," Phys. Rev. A **34**, 2185 (1986).
[18]E. A. Mason and E. W. McDaniel, *Transport Properties of Ions in Gases* (Wiley Online Library, 1988), Vol. 26.
[19]L. A. Viehland, "Velocity distribution functions and transport coefficients of atomic ions in atomic gases by a Gram—Charlier approach," Chem. Phys. **179**, 71 (1994).
[20]L. A. Viehland, *Gaseous Ion Mobility, Diffusion, and Reaction* (Springer, 2018), Vol. 105.
[21]D. A. Konovalov, D. G. Cocks, and R. D. White, "Unified solution of the Boltzmann equation for electron and ion velocity distribution functions and transport coefficients in weakly ionized plasmas," Eur. Phys. J. D **71**, 258 (2017).
[22]Z. Donkó, "Particle simulation methods for studies of low-pressure plasma sources," Plasma Sources Sci. Technol. **20**, 024001 (2011).
[23]K. Nanbu, "Probability theory of electron-molecule, ion-molecule, molecule-molecule, and Coulomb collisions for particle modeling of materials processing plasmas and cases," IEEE Trans. Plasma Sci. **28**, 971 (2000).
[24]S. Longo, "Monte Carlo models of electron and ion transport in non-equilibrium plasmas," Plasma Sources Sci. Technol. **9**, 468 (2000).
[25]R. Blackmore and B. Shizgal, "The role of pseudo-eigenvalues of the Boltzmann collision operator in thermalization problems," Can. J. Phys. **61**, 1038 (1983).
[26]B. Shizgal and R. Blackmore, "A discrete ordinate method of solution of linear boundary value and eigenvalue problems," J. Comput. Phys. **55**, 313 (1984).
[27]R. E. Robson, K. F. Ness, G. E. Sneddon, and L. A. Viehland, "Comment on the discrete ordinate method in the kinetic theory of gases," J. Comput. Phys. **92**, 213 (1991).
[28]K. Kumar, "Polynomial expansions in kinetic theory of gases," Ann. Phys. **37**, 113 (1966).
[29]D. Burnett, "The distribution of velocities in a slightly non-uniform gas," Proc. London Math. Soc. **s2-39**, 385 (1935).

[30]D. Burnett, "The distribution of molecular velocities and the mean motion in a non-uniform gas," Proc. London Math. Soc. **s2-40**, 382 (1936).
[31]C. Canuto, M. Y. Hussaini, A. Quarteroni, and T. A. Zang, *Spectral Methods: Evolution to Complex Geometries and Applications to Fluid Dynamics* (Springer Science & Business Media, 2007).
[32]L. Pareschi and B. Perthame, "A Fourier spectral method for homogeneous Boltzmann equations," Transp. Theory Stat. Phys. **25**, 369 (1996).
[33]L. Pareschi and G. Russo, "Numerical solution of the Boltzmann equation. I. Spectrally accurate approximation of the collision operator," SIAM J. Numer. Anal. **37**, 1217 (2000).
[34]F. Filbet and C. Mouhot, "Analysis of spectral methods for the homogeneous Boltzmann equation," Trans. Am. Math. Soc. **363**, 1947 (2011).
[35]G. H. Wannier, "Motion of gaseous ions in strong electric fields," Bell Syst. Tech. J. **32**, 170 (1953).
[36]L. A. Viehland and E. A. Mason, "Gaseous ion mobility in electric fields of arbitrary strength," Ann. Phys. **91**, 499 (1975).
[37]L. A. Viehland and E. A. Mason, "Gaseous ion mobility and diffusion in electric fields of arbitrary strength," Ann. Phys. **110**, 287 (1978).
[38]S. L. Lin, L. A. Viehland, and E. A. Mason, "Three-temperature theory of gaseous ion transport," Chem. Phys. **37**, 411 (1979).
[39]K. Kumar, "Talmi transformation for unequal-mass particles and related formulas," J. Math. Phys. **7**, 671 (1966).
[40]K. Kumar, "The Chapman-Enskog solution of the Boltzmann equation: A reformulation in terms of irreducible tensors and matrices," Aust. J. Phys. **20**, 205 (1967).
[41]R. E. Robson and K. F. Ness, "Velocity distribution function and transport coefficients of electron swarms in gases: Spherical-harmonics decomposition of Boltzmann's equation," Phys. Rev. A **33**, 2068 (1986).
[42]K. F. Ness, "Multi-term solution of the Boltzmann equation for electron swarms in crossed electric and magnetic fields," J. Phys. D: Appl. Phys. **27**, 1848 (1994).
[43]R. D. White, R. E. Robson, and K. F. Ness, "Computation of electron and ion transport properties in gases," Comput. Phys. Commun. **142**, 349 (2001).
[44]R. White, "Mass effects of light ion swarms in AC electric fields," Phys. Rev. E **64**, 056409 (2001).
[45]R. D. White, K. F. Ness, R. E. Robson, and B. Li, "Charged-particle transport in gases in electric and magnetic fields crossed at arbitrary angles: Multiterm solution of Boltzmann's equation," Phys. Rev. E **60**, 2231 (1999).
[46]R. D. White and R. E. Robson, "Multiterm solution of a generalized Boltzmann kinetic equation for electron and positron transport in structured and soft condensed matter," Phys. Rev. E **84**, 031125 (2011).
[47]S. Dujko, D. Bošnjaković, R. D. White, and Z. Lj Petrović, "Heating mechanisms for electron swarms in radio-frequency electric and magnetic fields," Plasma Sources Sci. Technol. **24**, 054006 (2015).
[48]R. E. Robson, M. J. Brunger, S. J. Buckman, G. Garcia, Z. L. Petrović, and R. D. White, "Positron kinetics in an idealized pet environment," Sci. Rep. **5**, 12674 (2015).
[49]S. Dujko, R. D. White, Z. L. Petrović, and R. E. Robson, "Benchmark calculations of nonconservative charged-particle swarms in dc electric and magnetic fields crossed at arbitrary angles," Phys. Rev. E **81**, 046403 (2010).
[50]L. C. Pitchford and A. V. Phelps, Comparative calculations of electron-swarm properties in N_2 at moderate $\frac{E}{N}$ values," Phys. Rev. A **25**, 540 (1982).
[51]A. V. Phelps and L. C. Pitchford, "Anisotropic scattering of electrons by N_2 and its effect on electron transport," Phys. Rev. A **31**, 2932 (1985).
[52]D. McMahon, "The Boltzmann equation theory of charged particle transport," Aust. J. Phys. **36**, 163 (1983).
[53]P. Segur, M.-C. Bordage, J.-P. Balaguer, and M. Yousfi, "The application of a modified form of the S_N method to the calculation of swarm parameters of electrons in a weakly ionised equilibrium medium," J. Comput. Phys. **50**, 116 (1983).
[54]M. Yousfi, P. Segur, and T. Vassiliadis, "Solution of the Boltzmann equation with ionisation and attachment: Application to SF_6," J. Phys. D: Appl. Phys. **18**, 359 (1985).
[55]S. Yachi, H. Date, K. Kitamori, and H. Tagashira, "A multi-term Boltzmann equation analysis of electron swarms in gases-the time-of-flight parameters," J. Phys. D: Appl. Phys. **24**, 573 (1991).
[56]K. F. Ness, "Spherical-harmonics decomposition of the Boltzmann equation for charged-particle swarms in the presence of both electric and magnetic fields," Phys. Rev. E **47**, 327 (1993).
[57]R. D. White, R. E. Robson, and K. F. Ness, "Nonconservative charged-particle swarms in AC electric fields," Phys. Rev. E **60**, 7457 (1999).
[58]D. Loffhagen and R. Winkler, "Time-dependent multi-term approximation of the velocity distribution in the temporal relaxation of plasma electrons," J. Phys. D: Appl. Phys. **29**, 618 (1996).
[59]D. Loffhagen and R. Winkler, "Multi-term treatment of the temporal electron relaxation in He, Xe and plasmas," Plasma Sources Sci. Technol. **5**, 710 (1996).
[60]R. Winkler, D. Loffhagen, and F. Sigeneger, "Temporal and spatial relaxation of electrons in low temperature plasmas," Appl. Surf. Sci. **192**, 50 (2002).
[61]D. Loffhagen and F. Sigeneger, "Advances in Boltzmann equation based modelling of discharge plasmas," Plasma Sources Sci. Technol. **18**, 034006 (2009).
[62]R. D. White, K. F. Ness, and R. E. Robson, "Development of swarm transport theory in radio-frequency electric and crossed electric and magnetic fields," Appl. Surf. Sci. **192**, 26 (2002).
[63]R. D. White, R. E. Robson, B. Schmidt, and M. A. Morrison, "Is the classical two-term approximation of electron kinetic theory satisfactory for swarms and plasmas?," J. Phys. D: Appl. Phys. **36**, 3125 (2003).
[64]M. Williams, *Mathematical Methods in Particle Transport Theory* (Butterworths, London, 1971).
[65]Z. L. Petrović, S. Dujko, D. Marić, G. Malović, Z. Nikitović, O. Sasić, J. Jovanović, V. Stojanović, and M. Radmilović-Radjenović, "Measurement and interpretation of swarm parameters and their application in plasma modelling," J. Phys. D: Appl. Phys. **42**, 194002 (2009).
[66]K. F. Ness and R. E. Robson, "Motion of muons in heavy hydrogen in an applied electrostatic field," Phys. Rev. A **39**, 6596 (1989).
[67]K. F. Ness and R. E. Robson, "Unified theoretical treatment of ion and electron transport properties in gases," in *Contributed Abstracts* (ICPIG XIX, Belgrade, 1989).
[68]F. Sigeneger and R. Winkler, "Response of the electron kinetics on spatial disturbances of the electric field in nonisothermal plasmas," Contrib. Plasma Phys. **36**, 551 (1996).
[69]G. J. M. Hagelaar and L. C. Pitchford, "Solving the Boltzmann equation to obtain electron transport coefficients and rate coefficients for fluid models," Plasma Sources Sci. Technol. **14**, 722 (2005).
[70]D. Trunec, Z. Bonaventura, and D. Nečas, "Solution of time-dependent Boltzmann equation for electrons in non-thermal plasma," J. Phys. D: Appl. Phys. **39**, 2544 (2006).
[71]G. J. Boyle, W. J. Tattersall, D. G. Cocks, R. P. McEachran, and R. D. White, "A multi-term solution of the space–time Boltzmann equation for electrons in gases and liquids," Plasma Sources Sci. Technol. **26**, 024007 (2017).
[72]J. C. Stephens, "A multi-term, multi-harmonic Boltzmann equation model for kinetic behavior in intense microwave and terahertz excited low temperature plasmas," Phys. Plasmas **25**, 103502 (2018).
[73]F. Sigeneger and R. Winkler, "On the mechanisms of spatial electron relaxation in nonisothermal plasmas," Plasma Chem. Plasma Process. **17**, 281 (1997).
[74]G. J. Boyle, M. J. E. Casey, D. G. Cocks, R. D. White, and R. J. Carman, "Thermalisation time of electron swarms in xenon for uniform electric fields," Plasma Sources Sci. Technol. **28**, 035009 (2019).
[75]J. de Urquijo, M. J. E. Casey, L. N. Serkovic-Loli, D. G. Cocks, G. J. Boyle, D. B. Jones, M. J. Brunger, and R. D. White, "Assessment of the self-consistency of electron–THF cross sections using electron swarm techniques: Mixtures of THF—Ar and THF—N_2," J. Chem. Phys. **151**, 054309 (2019).
[76]P. W. Stokes, D. G. Cocks, M. J. Brunger, and R. D. White, "Determining cross sections from transport coefficients using deep neural networks," Plasma Sources Sci. Technol. **29**, 055009 (2020).
[77]G. Boyle, W. J. Tattersall, D. Cocks, S. Dujko, and R. D. White, "Kinetic theory of positron-impact ionization in gases," Phys. Rev. A **91**, 052710 (2015).
[78]G. J. Boyle, M. J. E. Casey, R. D. White, and J. Mitroy, "Transport theory for low-energy positron thermalization and annihilation in helium," Phys. Rev. A **89**, 022712 (2014).
[79]D. G. Cocks, R. P. McEachran, G. J. Boyle, E. Cheng, and R. D. White, "Positron scattering and transport in liquid helium," J. Phys. B: At., Mol. Opt. Phys. **53**, 225201 (2020).

[80]S. Pancheshnyi, S. Biagi, M. C. Bordage, G. J. M. Hagelaar, W. L. Morgan, A. V. Phelps, and L. C. Pitchford, "The LXCat project: Electron scattering cross sections and swarm parameters for low temperature plasma modeling," Chem. Phys. **398**, 148 (2012), Chemical Physics of Low-Temperature Plasmas (in honour of Professor Mario Capitelli).
[81]L. C. Pitchford *et al.*, "LXCat: An open-access, web-based platform for data needed for modeling low temperature plasmas," Plasma Processes Polym. **14**, 1600098 (2017).
[82]R. Brandenburg, P. J. Bruggeman, and S. M. Starikovskaia, "Fast pulsed discharges," Plasma Sources Sci. Technol. **26**, 020201 (2017).
[83]G. J. Boyle, M. J. E. Casey, D. J. Cocks, R. D. White, and R. J. Carman, "Thermalisation time of electron swarms in helium and neon for uniform electric fields in the range 1 Td < E/N < 1000 Td," in Gaseous Electronics Meeting GEM XXI (ANU, Australia, 2020), publication in preparation.
[84]R. E. Robson and K. Kumar, "On the validity of the two-term approximation of the electron distribution function," Aust. J. Phys. **24**, 835 (1971).
[85]R. D. White *et al.*, "Electron transport in biomolecular gaseous and liquid systems: Theory, experiment and self-consistent cross-sections," Plasma Sources Sci. Technol. **27**, 053001 (2018).
[86]A. Filippelli, C. C. Lin, L. Anderson, and J. W. McConkey, "Principles and methods for measurement of electron impact excitation cross sections for atoms and molecules by optical techniques," Adv. At., Mol., Opt. Phys. **33**, 1–62 (1994).
[87]I. Bray and A. T. Stelbovics, "Convergent close-coupling calculations of electron-hydrogen scattering," Phys. Rev. A **46**, 6995 (1992).
[88]D. V. Fursa and I. Bray, "Calculation of electron-helium scattering," Phys. Rev. A **52**, 1279 (1995).
[89]M. C. Zammit, D. V. Fursa, and I. Bray, "Electron scattering from the molecular hydrogen ion and its isotopologues," Phys. Rev. A **90**, 022711 (2014).
[90]M. C. Zammit, J. S. Savage, D. V. Fursa, and I. Bray, "Complete solution of electronic excitation and ionization in electron-hydrogen molecule scattering," Phys. Rev. Lett. **116**, 233201 (2016).
[91]L. G. H. Huxley and R. W. Crompton, *Diffusion and Drift of Electrons in Gases* (John Wiley & Sons, 1974).
[92]R. Crompton, "Benchmark measurements of cross sections for electron collisions: Electron swarm methods," Adv. At., Mol., Opt. Phys. **33**, 97–148 (1994).
[93]Z. L. Petrović, M. Šuvakov, Ž. Nikitović, S. Dujko, O. Šašić, J. Jovanović, G. Malović, and V. Stojanović, "Kinetic phenomena in charged particle transport in gases, swarm parameters and cross section data," Plasma Sources Sci. Technol. **16**, S1 (2007).
[94]H. F. Mayer, "Über das verhalten von molekülen gegenüber freien langsamen elektronen," Ann. Phys. **369**, 451 (1921).
[95]C. Ramsauer, "Über den wirkungsquerschnitt der gasmoleküle gegenüber langsamen elektronen," Ann. Phys. **369**, 513 (1921).
[96]J. S. Townsend and V. A. Bailey, "The motion of electrons in argon," London, Edinburgh Dublin Philos. Mag. J. Sci. **43**, 593 (1922).
[97]A. G. Engelhardt and A. V. Phelps, "Elastic and inelastic collision cross sections in hydrogen and deuterium from transport coefficients," Phys. Rev. **131**, 2115 (1963).
[98]A. G. Engelhardt, A. V. Phelps, and C. G. Risk, "Determination of momentum transfer and inelastic collision cross sections for electrons in nitrogen using transport coefficients," Phys. Rev. **135**, A1566 (1964).
[99]R. D. Hake and A. V. Phelps, "Momentum-transfer and inelastic-collision cross sections for electrons in O_2, CO, and CO_2," Phys. Rev. **158**, 70 (1967).
[100]A. V. Phelps, "Rotational and vibrational excitation of molecules by low-energy electrons," Rev. Mod. Phys. **40**, 399 (1968).
[101]C. W. Duncan and I. C. Walker, "Collision cross-sections for low energy electrons in methane," J. Chem. Soc., Faraday Trans. 2 **68**, 1514 (1972).
[102]T. F. O'Malley and R. W. Crompton, "Electron-neon scattering length and S-wave phaseshifts from drift velocities," J. Phys. B: At. Mol. Phys. **13**, 3451 (1980).
[103]T. Taniguchi, M. Suzuki, K. Kawamura, F. Noto, and H. Tagashira, "A calculation method for estimating a cross section using a Boltzmann equation analysis," J. Phys. D: Appl. Phys. **20**, 1085 (1987).
[104]W. L. Morgan, "Use of numerical optimization algorithms to obtain cross sections from electron swarm data," Phys. Rev. A **44**, 1677 (1991).
[105]W. Morgan, "The feasibility of using neural networks to obtain cross sections from electron swarm data," IEEE Trans. Plasma Sci. **19**, 250 (1991).
[106]W. L. Morgan, "Test of a numerical optimization algorithm for obtaining cross sections for multiple collision processes from electron swarm data," J. Phys. D: Appl. Phys. **26**, 209 (1993).
[107]M. Brennan and K. Ness, "Momentum transfer cross section for e^-–Kr scattering," Aust. J. Phys. **46**, 249 (1993).
[108]G. E. Hinton, S. Osindero, and Y.-W. Teh, "A fast learning algorithm for deep belief nets," Neural Comput. **18**, 1527 (2006).
[109]G. E. Hinton and R. R. Salakhutdinov, "Reducing the dimensionality of data with neural networks," Science **313**, 504 (2006).
[110]Y. Bengio, P. Lamblin, D. Popovici, and H. Larochelle, "Greedy layer-wise training of deep networks," Adv. Neural Inf. Process. Syst. **19**, 153–160 (2006).
[111]M. Ranzato, C. Poultney, S. Chopra, and Y. Cun, "Efficient learning of sparse representations with an energy-based model," Adv. Neural Inf. Process. Syst. **19**, 1137–1144 (2006).
[112]H. Lee, C. Ekanadham, and A. Ng, "Sparse deep belief net model for visual area V2," Adv. Neural Inf. Process. Syst. **20**, 873–880 (2007).
[113]X. Glorot, A. Bordes, and Y. Bengio, "Deep sparse rectifier neural networks," in *Proceedings of the Fourteenth International Conference on Artificial Intelligence And Statistics* (JMLR Workshop and Conference Proceedings, 2011), pp. 315–323.
[114]G. Ruiz-Vargas, M. Yousfi, and J. de Urquijo, "Electron transport coefficients in the mixtures of H_2O with N_2, O_2, CO_2 and dry air for the optimization of non-thermal atmospheric pressure plasmas," J. Phys. D: Appl. Phys. **43**, 455201 (2010).
[115]J. de Urquijo, E. Basurto, A. M. Juárez, K. F. Ness, R. E. Robson, M. J. Brunger, and R. D. White, "Electron drift velocities in He and water mixtures: Measurements and an assessment of the water vapour cross-section sets," J. Chem. Phys. **141**, 014308 (2014).
[116]D. A. Dahl, T. H. Teich, and C. M. Franck, "Obtaining precise electron swarm parameters from a pulsed Townsend setup," J. Phys. D: Appl. Phys. **45**, 485201 (2012).
[117]P. Haefliger and C. M. Franck, "Detailed precision and accuracy analysis of swarm parameters from a pulsed Townsend experiment," Rev. Sci. Instrum. **89**, 023114 (2018).
[118]M. H. Hassoun *et al.*, *Fundamentals of Artificial Neural Networks* (MIT Press, 1995).
[119]A. Krogh, "What are artificial neural networks?," Nat. Biotechnol. **26**, 195 (2008).
[120]O. I. Abiodun, A. Jantan, A. E. Omolara, K. V. Dada, N. A. Mohamed, and H. Arshad, "State-of-the-art in artificial neural network applications: A survey," Heliyon **4**, e00938 (2018).
[121]G. Cybenko, "Approximation by superpositions of a sigmoidal function," Math. Control, Signals Syst. **2**, 303 (1989).
[122]K. Hornik, "Approximation capabilities of multilayer feedforward networks," Neural Networks **4**, 251 (1991).
[123]R. D. White, M. J. Brunger, N. A. Garland, R. E. Robson, K. F. Ness, G. Garcia, J. de Urquijo, S. Dujko, and Z. L. Petrović, "Electron swarm transport in THF and water mixtures," Eur. Phys. J. D **68**, 125 (2014).
[124]M. U. Bug, W. Yong Baek, H. Rabus, C. Villagrasa, S. Meylan, and A. B. Rosenfeld, "An electron-impact cross section data set (10 eV–1 keV) of DNA constituents based on consistent experimental data: A requisite for Monte Carlo simulations," Radiat. Phys. Chem. **130**, 459 (2017).
[125]E. Alizadeh, T. M. Orlando, and L. Sanche, "Biomolecular damage induced by ionizing radiation: The direct and indirect effects of low-energy electrons on DNA," Annu. Rev. Phys. Chem. **66**, 379 (2015).
[126]M. C. Fuss, A. G. Sanz, F. Blanco, P. Limão-Vieira, M. J. Brunger, and G. García, "Differential and integral electron scattering cross sections from tetrahydrofuran (THF) over a wide energy range: 1–10 000 eV," Eur. Phys. J. D **68**, 161 (2014).
[127]L. Sanche, "Low energy electron-driven damage in biomolecules," Eur. Phys. J. D **35**, 367 (2005).
[128]M. J. Brunger, "Electron scattering and transport in biofuels, biomolecules and biomass fragments," Int. Rev. Phys. Chem. **36**, 333 (2017).

[129]N. A. Garland, M. J. Brunger, G. Garcia, J. de Urquijo, and R. D. White, "Transport properties of electron swarms in tetrahydrofuran under the influence of an applied electric field," Phys. Rev. A **88**, 062712 (2013).
[130]M. Casey, J. De Urquijo, L. Serkovic Loli, D. Cocks, G. Boyle, D. Jones, M. Brunger, and R. White, "Self-consistency of electron-THF cross sections using electron swarm techniques," J. Chem. Phys. **147**, 195103 (2017).
[131]P. W. Stokes, M. J. Casey, D. G. Cocks, J. de Urquijo, G. García, M. J. Brunger, and R. D. White, "Self-consistent electron–THF cross sections derived using data-driven swarm analysis with a neural network model," Plasma Sources Sci. Technol. **29**, 105008 (2020).
[132]M. C. Fuss *et al.*, "Electron interactions with tetrahydrofuran," J. Phys.: Conf. Ser. **373**, 012010 (2012).
[133]K. Aflatooni, A. M. Scheer, and P. D. Burrow, "Total dissociative electron attachment cross sections for molecular constituents of DNA," J. Chem. Phys. **125**, 054301 (2006).
[134]R. Janečková, O. May, A. Milosavljević, and J. Fedor, "Partial cross sections for dissociative electron attachment to tetrahydrofuran reveal a dynamics-driven rich fragmentation pattern," Int. J. Mass Spectrom. **365-366**, 163 (2014).
[135]S. F. Biagi, Biagi database (Magboltz version 7.1), www.lxcat.net/Biagi-v7.1 (2004); accessed 05 December 2022.
[136]S. Kawaguchi and T. Murakami, "Physics-informed neural networks for solving the Boltzmann equation of the electron velocity distribution function in weakly ionized plasmas," Jpn. J. Appl. Phys. **61**, 086002 (2022).
[137]S. Kawaguchi, K. Takahashi, H. Ohkama, and K. Satoh, "Deep learning for solving the Boltzmann equation of electrons in weakly ionized plasma," Plasma Sources Sci. Technol. **29**, 025021 (2020).
[138]R. Robson, R. D. White, and M. A. Morrison, "Some fundamental questions concerning the kinetic theory of electrons in molecular gases and the e–H_2 vibrational cross section controversy," J. Phys. B: At., Mol. Opt. Phys. **36**, 4127 (2003).
[139]D. G. Cocks, personal communication (2022).